Journal of Magnetic Resonance 194 (2008) 192–201

Contents lists available at ScienceDirect

Journal of Magnetic Resonance

journal homepage: www.elsevier.com/locate/jmr

Spin-selective multiple quantum excitation: Relative signs of the couplings and ambiguous situations

Sankeerth Hebbar [a,b], N. Suryaprakash [b,*]

[a] Solid State and Structural Chemistry Unit, Indian Institute of Science, Bengaluru, Karnataka 560 012, India
[b] NMR Research Centre, Indian Institute of Science, Bengaluru, Karnataka 560 012, India

ARTICLE INFO

Article history:
Received 25 February 2008
Revised 28 June 2008
Available online 4 July 2008

Keywords:
Multiple quantum
Spin state selection
Sign of the couplings
Dipolar couplings
Scalar couplings

ABSTRACT

Homonuclear higher quantum NMR spectra of heteronuclear spin systems result in fewer transitions aiding the analyses. In such experiments the spin states of the heteronuclei do not get disturbed in both single and multiple quantum dimensions resulting in the separation of active homonuclear and passive heteronuclear couplings in two dimensions. The cross sections of the single-quantum dimension get displaced according to the strengths of the passive couplings. The directions of the displacement of these cross sections provide relative signs among the passive couplings. The present study demonstrates the situations when the displacement vectors, though provide the relative signs, could be ambiguous. The dynamics of the spin systems in homo- and heteronuclear multiple quantum studies have been discussed using polarization operator approach. The experimental results on ^{13}C- and ^{15}N-labeled isotopomers of acetonitrile, in both isotropic and thermotropic liquid crystalline phases, are reported.

1. Introduction

Determination of the relative signs of the direct and indirect couplings is one of the widely studied areas in NMR [1]. Several one and two dimensional NMR techniques are available in the literature for the determination of magnitudes and relative signs of the coupling constants, such as, Z-COSY, Soft-COSY, E-COSY [2–6], spin tickling [7] and, double and triple resonance [8] experiments. The spin state-selective detection is another direction of approach where the high-field and low-field components of the multiplet are separated or individually detected [9–24]. Two-dimensional experiments correlating homonuclear spin-selective higher quantum to single quantum also provided the relative signs of the couplings in weakly scalar-coupled spin systems [25,26]. However, these multiple quantum experiments fail to provide the information about the relative signs of the homonuclear or active couplings. In the present work the different combination of homo- and heteronuclear multiple quantum experiments have been carried out on weakly coupled spin systems to derive this information. Relative signs of all the indirect and direct dipolar couplings have been determined, respectively, in isotropic and liquid crystalline phases, in doubly ^{13}C- and ^{15}N-labeled acetonitrile. Furthermore, it is also demonstrated that in systems containing two different heteronuclei, the spectral complexity can be reduced by mimicking simultaneous decoupling of two different heteronuclei or the selective decoupling of one of the heteronucleus. This has been achieved by employing the homonuclear highest quantum or the spin-selective heteronuclear higher quantum detection. The ambiguous situations encountered in obtaining the relative signs of the couplings are discussed using the polarization operator approach. The results have been confirmed experimentally both in scalar- and dipolar-coupled spin systems. The relative signs of the scalar couplings thus determined have been employed to obtain the precise magnitudes and relative signs of the dipolar couplings.

2. Experimental

The different isotopomers of doubly labeled acetonitrile, viz., $^{13}CH_3{}^{13}CN$ (**1**), $^{13}CH_3C^{15}N$ (**2**), $CH_3{}^{13}C^{15}N$ (**3**) and $^{13}CH_3{}^{13}C^{15}N$ (**4**) obtained from Sigma–Aldrich were used without further purification. The solution of isotopomer **4** in $CDCl_3$ was used for the studies in isotropic phase. For studies in the aligned media the solution of isotopomer **1** was prepared in the liquid crystal ZLI-1132 (mixture of three phenyl cyclohexanes and one bicyclohexane) and the solutions of the remaining isotopomers were prepared in the liquid crystal ZLI-1115 (*trans*-4-heptyl-1-(4-cyanophenyl)-cyclohexane). The liquid crystals were obtained from MERCK. The proton spectra provided the line widths of less than 0.5 and 5.0 Hz in isotropic and liquid crystalline phases respectively. All the experiments were carried out on a Bruker AV-500 NMR spectrometer with field strength of 11.74 T operating at the frequencies of 500.13, 125.77 and 50.67 MHz for ^1H, ^{13}C and ^{15}N nuclei, respectively. The tem-

* Corresponding author. Fax: +91 80 2360 1550.
E-mail address: nsp@sif.iisc.ernet.in (N. Suryaprakash).

1090-7807/$ - see front matter © 2008 Elsevier Inc. All rights reserved.
doi:10.1016/j.jmr.2008.07.001

perature was maintained at 300 K by a Bruker BVT-3000 temperature-regulating system.

All the homo- and heteronuclear two-dimensional multiple quantum (MQ)– single quantum (SQ) correlation experiments were carried out using the pulse sequences given in Fig. 2A and B, respectively. The delays, τ, were optimized to get anti-phase magnetization before the application of a second 90° pulse. The 180° pulses between the two $\pi/2$ pulses ensure that the chemical shift evolution is refocused. The second 90° pulse converts the anti-phase magnetization into MQ coherence. Any particular order of the MQ to SQ coherence transfer is selected by applying the gradients and the last 90° pulse converts the MQ coherence into observable SQ coherence. Two-dimensional data were processed with sine bell and exponential window functions in F_1 and F_2 dimensions, respectively, with zero filling to twice the time domain data points in both the dimensions. The acquisition and processing parameters are reported in the corresponding figure captions.

3. Multiple quantum spin state selection and relative signs of couplings

The allowed transitions in a particular higher quantum depend on the number of active spins and their interaction with the passive spins [27–29]. The different MQ orders of N interacting spins can be selectively excited or detected [30]. In a coupled spin system with several possibilities of higher quantum order, the particular order of coherence can be selectively or non-selectively excited. In a non-selective excitation, the cross section taken along the SQ dimension for each spin state of the passive spin in the MQ dimension, provides all the transitions expected in the SQ dimension. In a selective excitation only the spin states of active spins are disturbed and the states of passive spins remain unperturbed in both MQ and SQ dimensions. Each state of the passive spins in the MQ dimension then encodes the spin states involved in the SQ transitions that arise only due to coupling between active spins. The cross section taken along SQ dimension corresponding to any one of the passive spin states results in the selective detection of very few SQ transitions, but suffice for the determination of the couplings between the active spins. The number of SQ transitions in the one-dimensional spectrum, which are generally redundant, is thus significantly reduced thereby simplifying the complexity spectrum, as far as the determination of the couplings among the active spins are concerned. Furthermore, the F_1 cross sections are displaced based on the strengths of the passive couplings. The directions of the tilt of the displacement vectors provide information on the relative signs of the passive couplings. This phenomenon has been understood using product operator approach [26].

4. Results and discussion

4.1. Analyses ^1H and ^{13}C spectra of acetonitrile oriented in liquid crystal

The proton and ^{13}C-detected NMR spectra of all the isotopomers are amenable for the first-order analyses both in isotropic and oriented phases. The isotopomers, **1**, **2** and **3**, form A_3MX type of spin systems, where A_3 pertains to three methyl protons, M and X pertains to ^{13}C or ^{15}N depending on the isotopomer. However, the spin system in the isotopomer **4** is of the type A_3MPX, where A_3 corresponds to three methyl protons, M, P and X are two ^{13}C spins and one ^{15}N spin, respectively. The SQ spectrum of spin A in A_3MX spin system (**1**, **2** and **3**) results in a 1:2:1 triplet due to D_{HH}. Each transition of this triplet is further split into doublet of a doublet of equal intensity, due to D_{CH} and/or D_{NH}, giving rise to 12 transitions. Similarly in **4**, there are 24 transitions as each of these 12 transitions is further split by the third spin (^{15}N or ^{13}C). The first-order analyses of the spectra of the isotopomers provide the values of D_{12}, T_{14}, T_{15} and T_{16} (where $T_{ij} = J_{ij} + 2D_{ij}$). In the isotropic phase, except for the non-appearance of the splitting pattern among methyl protons and the influence of J couplings instead of dipolar couplings, the nomenclature of the spin system is identical to that in the liquid crystalline phase.

The chemical structure with the numbering of the nuclei and ^1H and ^{13}C spectra of isotopomer **4** are shown in Fig. 1. The M- or X-detected SQ spectrum of **1** gave the doublet of a quartet at the chemical shift positions of carbon 4 and the signal from the carbon attached to nitrogen (C_5) is significantly broadened due to directly bonded quadrupolar ^{14}N spin. The couplings T_{14} and T_{45}, could be determined from this spectrum. The M- and X-detected spectrum of **2** and **3** are doublet of quartets at the chemical shift positions of M or X giving T_{14}, T_{15}, T_{46} and T_{56}. The spectrum of **4** provides a quartet at the chemical shift positions of each carbon due to T_{CH} which are further split into doublet of a doublet from the remaining ^{13}C and ^{15}N spins. The ^{15}N labeling aided the detection of sharp resonances for C_5 carbon in isotopomers **3** and **4**. The multiplicity at the chemical shift position of carbon 4, provides T_{14}, T_{45} and T_{46}, whereas the multiplicity at the chemical shift position of carbon 5 provides T_{15}, T_{45} and T_{56}. Thus from both ^1H and ^{13}C spectra of **4**, it is possible to determine all the seven couplings, viz., D_{12}, T_{14}, T_{15}, T_{16}, T_{45}, T_{46} and T_{56}. The ^{15}N spectra of **2**, **3** and **4** provide the redundant information.

4.2. Reducing the redundancy: mimicking simultaneous decoupling of all the heteronuclei

To reduce the redundancy of single-quantum transitions of the one-dimensional proton spectrum and to determine the relative signs of the couplings, we have employed our earlier developed methods [25,26]. The homonuclear ^1H triple-quantum (3Q) spectra of all the isotopomers were recorded, but the present discussion will be restricted to 3Q spectra of **4** reported in Fig. 3. The discussion for other isotopomers is a mere extension of the analogy.

In the 3Q spectra of isotopomer **4**,the passive spins, M, P and X, are the two ^{13}C spins and one ^{15}N spin, respectively. This results in eight identifiable transitions in the MQ dimension corresponding to eight passive spin states $|M_\alpha P_\alpha X_\alpha\rangle$, $|M_\alpha P_\alpha X_\beta\rangle$, $|M_\alpha P_\beta X_\alpha\rangle$, $|M_\alpha P_\beta X_\beta\rangle$, $|M_\beta P_\alpha X_\alpha\rangle$, $|M_\beta P_\alpha X_\beta\rangle$, $|M_\beta P_\beta X_\alpha\rangle$ and $|M_\beta P_\beta X_\beta\rangle$. The separations giving the coupling information are marked in the figure. The cross sections taken parallel to the SQ dimension corresponding to each of the eight spin states of **4** in the 3Q dimension results in a triplet, which are displaced along the F_1 dimension. The separation of the adjacent transitions of the triplet in each cross section provides the dipolar coupling among the methyl protons. Although the F_2 projection resemble the normal one-dimensional spectrum, the transitions detected according to the spin states of the passive spins mimic the simultaneous decoupling of protons from both ^{13}C and ^{15}N. Nevertheless, the coupling information between the protons and coupled heteronuclei is derivable from the 3Q dimension. Thus the method can be employed for simplification of the one-dimensional spectra, when different heteronuclei are present, as far as the determination of the homonuclear couplings is concerned. Irrespective of the fact whether the spin system is strongly or weakly coupled and whether spins are scalar or dipolar coupled, the technique mimics the decoupling of all the heteronuclei simultaneously. Similar discussion can also be extended to the ^1H 3Q–SQ correlation spectra of other isotopomers.

The direction of tilt of the cross sections along the F_1 dimension indicates that all the passive couplings have the same signs. The magnitudes and of the couplings obtained by the analysis of the homonuclear proton 3Q spectrum are reported in Table 1. The

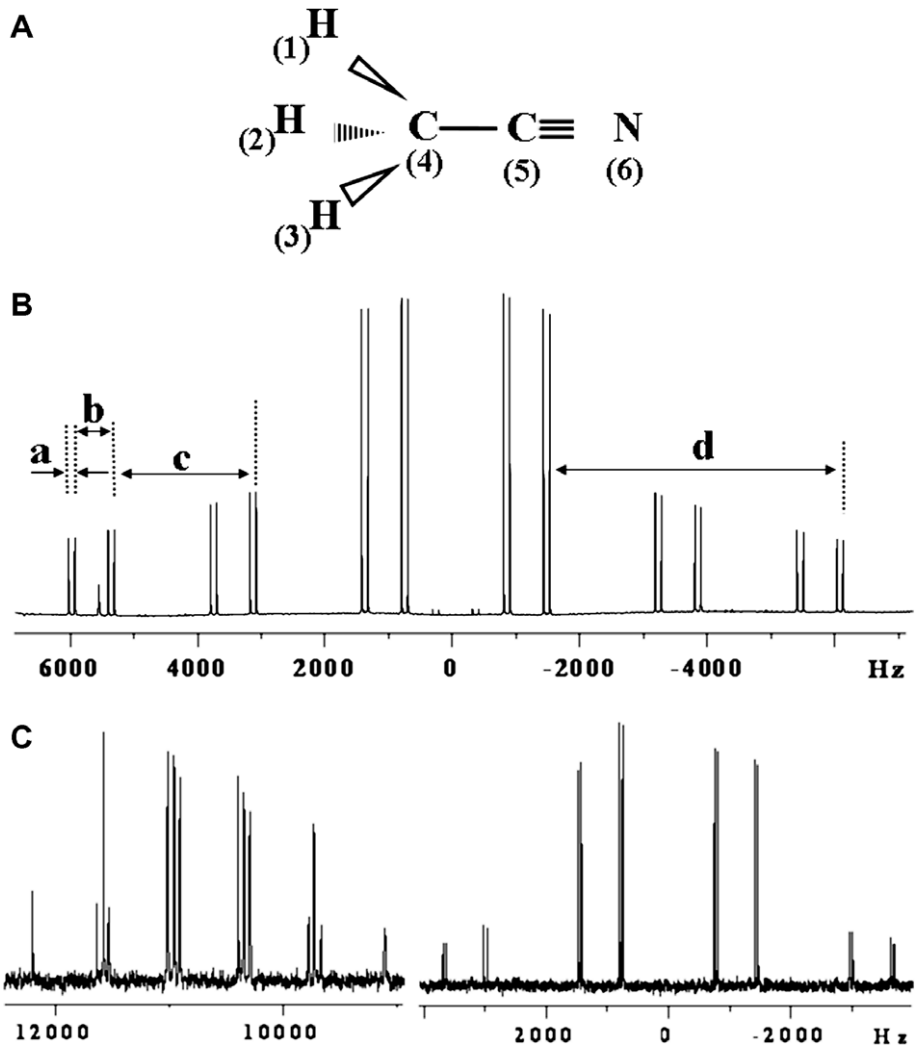

Fig. 1. (A) The chemical structure and numbering of interacting spins in doubly labeled acetonitrile; (B and C) ^{1}H and ^{13}C spectra of isotopomer $^{13}CH_3{}^{13}C^{15}N$, respectively. The marked separations a–d provide coupling information T_{16}, T_{15}, T_{14} and T_{12} ($3D_{HH}$), respectively.

analyses of homonuclear 3Q–SQ spectra of the remaining isotopomers also gave identical information on the relative signs of the couplings.

4.3. Mimicking selective decoupling: heteronuclear 4Q experiments

The simultaneous flipping of three methyl protons and a heteronucleus results in fourth quantum (4Q) spectrum. In **1**, two 4Q spectra, viz., A_3M and A_3X could be simultaneously detected and in **2** and **3**, depending on the isotopomer two types of 4Q excitations, viz., A_3M and A_3X are possible. In the isotopomers **1**, **2** and **3**, the 4Q dimension pertains to the spin system of the type AX, where A is the super spin with three protons and any one of the two heteronuclei flipping simultaneously and X is the passive spin. Projection on the 4Q dimension is A part of AX spin system and is a doublet corresponding to the two spin states $|\alpha\rangle$ and $|\beta\rangle$ of the X spin with the separation giving the sum of all the passive couplings. In **1**, the excitation of either of the two possible 4Q disturbs the spin states of the non-participating ^{13}C spin and does not achieve any spin state selection and the question of discussing the relative signs of the couplings from the displacement vectors does not arise. This is equivalent to a non-selective 4Q excitation. The simultaneously detected two 4Q spectra of **1** are reported in Fig. 4. The cross section taken parallel to SQ dimension, corresponding to each of the spin states $|\alpha\rangle$ and $|\beta\rangle$ in the 4Q dimension for either carbon numbered 4 or 5, results in doublet of a triplet from which D_{HH}, T_{14} and T_{15} can be derived and are marked in the figure.

In the A_3M 4Q spectra of **2** reported in Fig. 5A, the doublet separation in the 4Q dimension provides the sum of the passive couplings, T_{16} and T_{46}. The projection taken along SQ dimension provides doublet of doublet of a triplet. These 12 transitions get displaced in the 4Q dimension according to two spin states $|\alpha\rangle$ and $|\beta\rangle$ of ^{15}N. The cross section taken for any spin state in the 4Q dimension provides doublet of a triplet. This is a situation where ^{15}N is selectively decoupled in each cross section. The derivable couplings D_{HH}, T_{14} and T_{16} are marked in the figure. Similarly, in the A_3X 4Q spectra of **2** reported in Fig. 5b, the derivable couplings, D_{HH}, T_{16} and T_{46} are marked with alphabets and their values are reported in Table 1. This is a situation where ^{13}C spins are selectively decoupled in each cross section. The twelve transitions are displaced in the 4Q dimension according to the spin states of ^{13}C.

The analogy of the analyses can be suitably extended to all the 4Q spectra of the remaining isotopomers. In isotopomer **4** there are three possible 4Q spectra, viz., A_3M, A_3P and A_3X, where M, P and X pertain to the spins numbered 4, 5 and 6, respectively. However, the present discussion is restricted to one of these three possibilities. For each 4Q spectrum, 4Q dimension pertains to the A part of

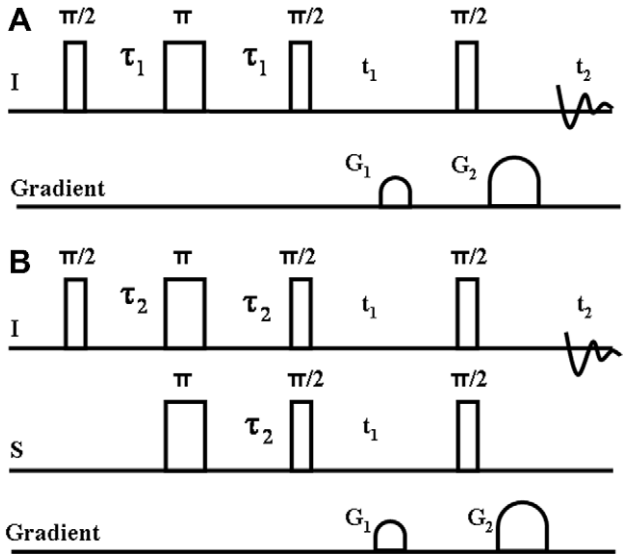

Fig. 2. (A and B) The pulse sequences used for the excitation of homo- and heteronuclear experiments used in all the experiments. The phases of all the pulses are set to x and the selection of the particular quantum coherence is achieved by the gradients. G_1 and G_2 are the gradients used to selectively detect the particular order of the quantum.

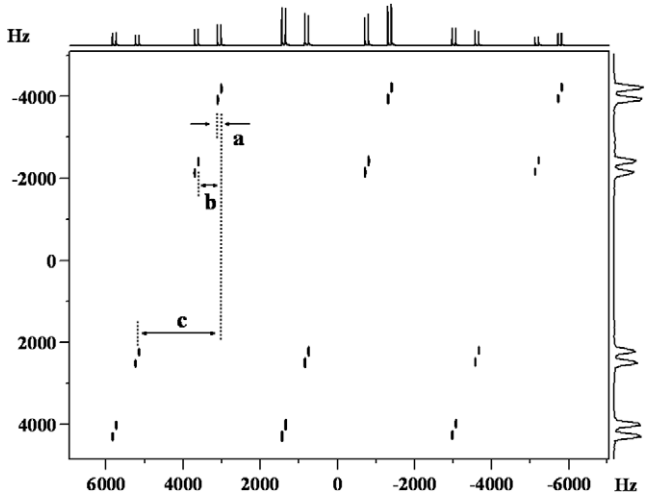

Fig. 3. The homonuclear 3Q–SQ correlation spectra of isotopomer **4**. The t_1 and t_2 dimensions corresponds to 3Q and SQ dimensions, respectively. The size of the 2D data matrix is 128 × 8k. Eight scans for each FID with a recycle delay of 3 s. The optimized τ delay is 0.056 ms. Digital resolution is 25 and 1.0 Hz in F_1 and F_2 dimensions, respectively. $|\alpha\alpha\alpha\rangle$, $|\alpha\alpha\beta\rangle$, $|\alpha\beta\alpha\rangle$, $|\alpha\beta\beta\rangle$, $|\beta\alpha\alpha\rangle$, $|\beta\alpha\beta\rangle$, $|\beta\beta\alpha\rangle$ and $|\beta\beta\beta\rangle$ are the eight spin states corresponding to two ^{13}C and ^{15}N spins. The alphabets marked a–d provide coupling information, $3D_{12}$, T_{14}, T_{15} and T_{16}, respectively.

an AMX spin system with four passive spin states. For A_3X 4Q spectrum reported in Fig. 6, the four possible spin states in the 4Q dimension are $|M\alpha P\alpha\rangle$, $|M\alpha P\beta\rangle$, $|M\beta P\alpha\rangle$ and $|M\beta P\beta\rangle$. The separations providing four different couplings are marked in the figure. However, there is a spin state selection due to ^{13}C spins and also the displacement of cross sections.

4.4. Relative signs of the couplings from MQ separations

Since MQ terms evolve during t_1 as a sum of all the passive couplings the frequency separations can be exploited for deriving the relative signs of the passive couplings. The signs of T_{14} and T_{15} with respect to T_{CC} are obtainable from the heteronuclear 4Q (A_3M and A_3X) of **1**, wherein the three protons of the methyl group, the methyl carbon and the carbonyl carbon are excited (Fig. 4). The larger splitting (6300 Hz) marked **e** in the spectrum corresponds to $3(T_{14}) \pm T_{45}$ and the smaller splitting (2710 Hz) marked **d** corresponds to $3(T_{15}) \pm T_{45}$. From the one-dimensional spectrum we have the values of $3D_{HH}$ (4830 Hz), T_{14} (2330 Hz), T_{15} (650 Hz) and T_{45} (710 Hz). (It is to be noted that sample **1** was in a different solvent and therefore the magnitudes are different from Table 1). Algebraic combination of these couplings provides the information that T_{14} and T_{CC} have opposite signs and the couplings T_{15} and T_{CC} have same signs. In addition the heteronuclear 3Q experiment (not shown), where two protons and the methyl carbon were excited, reveals that T_{45} is opposite in sign to that of D_{HH}.

Similarly splitting along 4Q dimension in 4Q spectrum of **2** (Fig. 5b), wherein three protons of the methyl group and Nitrogen (N_6) are excited, provides the information that, T_{14} and T_{46} are of opposite signs. Splitting along 3Q dimension in 3Q spectrum of **2** (not shown), wherein two protons of the methyl group and Nitrogen (N_6) are excited, provides the information that D_{HH} and T_{16} are of opposite signs. Splitting along 3Q dimension in 3Q spectrum of **3**(not shown), wherein two protons of the methyl group and Nitrogen (N_6) are excited, reveals that T_{16} and T_{56} have same signs.. The relative signs of the couplings derived by the combination of all these experiments are summarized in Table 1.

These observations contradict what was inferred from the homonuclear 3Q experiments that the relative signs of all the couplings are identical. Such ambiguous situations are encountered in homonuclear 3Q spectra of all the four isotopomers. This implies that the directions of the displacement vectors cannot always be taken as an indicator for the determination of the relative signs of the couplings. To unravel this ambiguity, the dynamics of the spin system during the pulse sequence is understood using the polarization operator approach [31] and is discussed in the following section.

4.5. Spin dynamics in homonuclear 3Q–SQ correlation

The behavior of the magnetization during both t_1 and t_2 periods is discussed for the isotopomer **4**, an A_3MPX spin system. The discussion is equally valid for understanding the dynamics of the remaining isotopomers. In the homonuclear 3Q–SQ correlation, the two triple-quantum states for the super spin A in the t_1 dimension corresponds to $|\alpha\alpha\alpha\rangle$ and $|\beta\beta\beta\rangle$. The coherence between these two states is represented as $A_{1+}A_{2+}A_{3+}$, where A_{i+} is the raising operator given as $A_{i+} = A_{ix} + A_{iy}$. Therefore, the polarization operator during the t_1 period can be written as $A_{1+}A_{2+}A_{3+}M_iP_jX_k$, where i, j and k represent any of the $|\alpha\rangle$ and $|\beta\rangle$ states of the spins M, P and X, respectively. Pertaining to eight product spin states of the passive spins, there are eight transitions along the F_1 dimension. The application of the second 90° pulse converts these 3Q terms into SQ terms. As an example, the 3Q term $A_{1+}A_{2+}A_{3+}$ coupled to one of the passive spin states, viz., $M\alpha P\alpha X\alpha$ gets converted to A_- single quantum term as;

$$\begin{aligned} A_{1+}A_{2+}A_{3+}M_\alpha P_\alpha X_\alpha \rightarrow\ & A_{1-}A_{2\alpha}A_{3\alpha}M_\alpha P_\alpha X_\alpha \\ & A_{1-}A_{2\alpha}A_{3\beta}M_\alpha P_\alpha X_\alpha \\ & A_{1-}A_{2\beta}A_{3\alpha}M_\alpha P_\alpha X_\alpha \\ & A_{1-}A_{2\beta}A_{3\beta}M_\alpha P_\alpha X_\alpha. \end{aligned} \quad (1)$$

The second and third terms of Eq. (1) have the same frequency and the four terms gives rise to a triplet for all the combinations of passive spin states. Similarly, the conversion of the triple-quantum coherence coupled to all the passive spin states can be calculated and are summarized in Table 2. Thus there are 24 allowed transi-

Table 1
The magnitudes and signs of the scalar and dipolar couplings determined by the combination of homo- and heteronuclear MQ–SQ correlation experiments on different isotopomer of doubly labeled acetonitrile

Spins	Couplings (T_{ij}) in oriented media (Hz)		Indirect couplings (J_{ij}) (Hz)	Direct couplings (D_{ij})	
	Conventional[a]	Adopting sign of gyromagnetic ratio		Experimental (Hz)	From fixed geometry[b] (Hz)
HHH	+4575	+4575			
C_4H	+2214	+2214	+136	+1039	+1042
C_5H	−620	−620	−10	−305	−292
C_4C_5	−667	−667	+58	−363	−356
N_6H	−96	+96	−1.8	+47	+48
N_6C_4	−54	+54	+2.8	+26	+26
N_6C_5	−528	+528	+18	+255	+318[c]

[a] Without considering the sign of the gyro-magnetic ratio.
[b] With the assumption that, $^3D_{HH}$ = +4575, fixed geometry, and single-order parameter.
[c] Attempt was to determine only the correct signs and not the precise magnitudes.

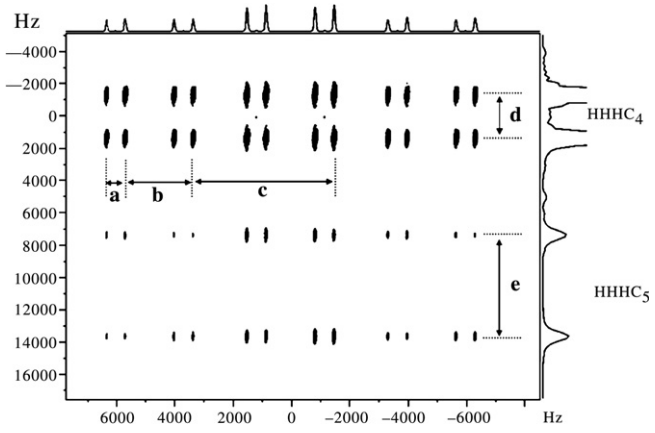

Fig. 4. The heteronuclear A_3M and A_3X 4Q spectrum of isotopomer **1**. The t_1 and t_2 dimensions corresponds to 4Q and SQ dimensions. The size of the 2D data matrix is 128 × 8k. Sixteen scans for each FID was accumulated with a recycle delay of 3 s. The optimized τ delay is 0.12 ms. Digital resolution is 50.0 and 1.0 Hz in F_1 and F_2 dimensions, respectively. $|\alpha\rangle$ and $|\beta\rangle$ are the two spin states of the passive ^{13}C spin and are marked for both carbons 4 and 5. The separations (in Hz) marked d and e at the chemical shift positions of carbon 4 and 5, respectively, provide the sum of passive couplings. The other separations marked are (a) T_{15}, (b) T_{14} and (c) $3D_{12}$.

tions in the F_2 dimension, that are displaced along the F_1 dimension corresponding to eight passive spin states.

The appearance of the homonuclear 3Q–SQ correlation spectrum for different sign combinations of passive couplings can easily be depicted by the pictorial representation of the two-dimensional matrix. With an initial assumption that all the passive couplings have same sign, the appearance of the spectrum is illustrated in Fig. 7A. The eight transitions in the 3Q dimension depicted are from the eight possible combination of spin states of M, P and X which are marked along the 3Q dimension. In the SQ dimension there are 24 proton transitions arising from the splitting of triplet of methyl protons by the eight spin states of M, P and X as depicted in the figure.

The Fig. 7B represents the 2D matrix when the signs of T_{15} and T_{16} are reversed. This pertains to a situation when the spin states $|\alpha\rangle$ and $|\beta\rangle$ of P spin are interchanged in both 3Q and SQ dimensions. Both the figures are identical in appearance, including the directions of displacements, indicating that the change of signs of the couplings does not alter the appearance of 3Q–SQ correlated spectrum. This is true for change of signs for any combination of the passive couplings. The implication of these observations is that it is not possible to arrive at the relative signs of the couplings by employing the direction of tilt of the displacement vectors in homonuclear 3Q–SQ correlation experiments.

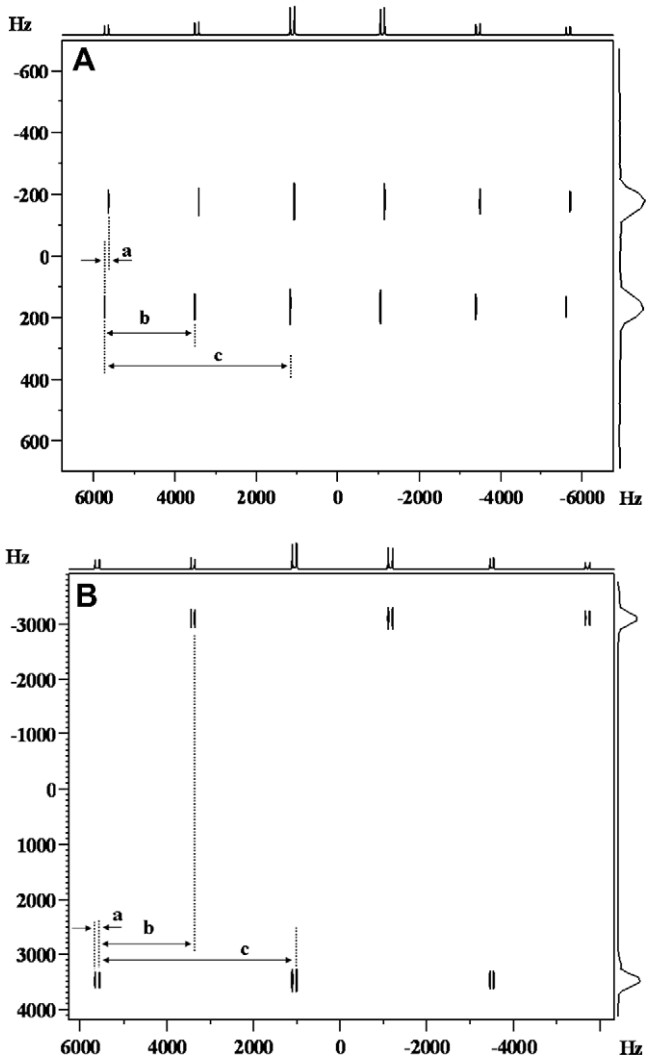

Fig. 5. (A) The heteronuclear A_3M 4Q spectrum of isotopomer **2**. The t_1 and t_2 dimensions corresponds to 4Q and SQ dimensions. The 2D data matrix is 64 × 8k. Sixteen scans for each FID were accumulated and a recycle delay of 3 s. The optimized τ delay is 0.15 ms. Digital resolution is 23.0 and 1.0 Hz in F_1 and F_2 dimensions, respectively. $|\alpha\rangle$ and $|\beta\rangle$ are the two spin states of the passive ^{15}N spin. The separations (in Hz) provide (a) T_{16}, (b) T_{14} and (c) $3D_{HH}$. (B) The heteronuclear A_3X 4Q spectrum of isotopomer **2**. The t_1 and t_2 dimensions corresponds to 4Q and SQ dimensions. The 2D data matrix is 64 × 8k. Sixteen scans for each FID were accumulated with a recycle delay of 3 s. The optimized τ delay is 0.4 ms. Digital resolution was 78.0 and 1.0 Hz in F_1 and F_2 dimensions, respectively. $|\alpha\rangle$ and $|\beta\rangle$ are the two spin states of the passive ^{13}C spin. The separations (in Hz) providing coupling information are (a) T_{16}, (b) T_{14} and (c) $3D_{HH}$.

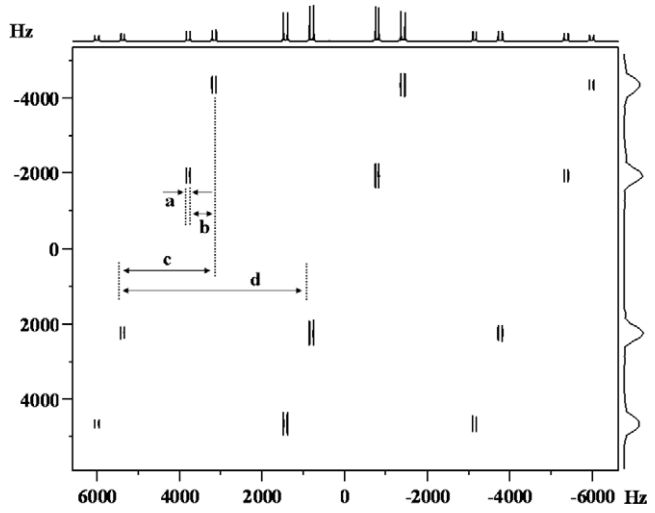

Fig. 6. The heteronuclear A_3X 4Q spectrum of isotopomer **4**. The t_1 and t_2 dimensions corresponds to 4Q and SQ dimensions. The 2D data matrix is 64 × 8k. Sixteen scans for each FID was accumulated with a recycle delay of 5 s. The optimized τ delay is 2.6 ms. Digital resolution is 25.0 and 1.0 Hz in F_1 and F_2 dimensions, respectively. $|\alpha\alpha\rangle$, $|\alpha\beta\rangle$, $|\beta\alpha\rangle$ and $|\beta\beta\rangle$ are the four passive spin states of carbons. The separations (in Hz) provide (a) T_{16}, (b) T_{14}, (c) T_{15} and (d) $3D_{HH}$.

Table 2
Evolution of the terms in the homonuclear 3Q–SQ correlation experiment in an A_3MPX spin system

t_1 period (3Q)						t_2 period (SQ)					
A_1	A_2	A_3	M	P	X	A_1	A_2	A_3	M	P	X
A_{1-}	A_{2-}	A_{3-}	M_α	P_α	X_α	A_{1-}	$A_{2\alpha}$	$A_{3\alpha}$	M_α	P_α	X_α
A_{1-}	A_{2-}	A_{3-}	M_α	P_α	X_β	A_{1-}	$A_{2\alpha}$	$A_{3\alpha}$	M_α	P_α	X_β
A_{1-}	A_{2-}	A_{3-}	M_α	P_β	X_α	A_{1-}	$A_{2\alpha}$	$A_{3\alpha}$	M_α	P_β	X_α
A_{1-}	A_{2-}	A_{3-}	M_α	P_β	X_β	A_{1-}	$A_{2\alpha}$	$A_{3\alpha}$	M_α	P_β	X_β
A_{1-}	A_{2-}	A_{3-}	M_β	P_α	X_α	A_{1-}	$A_{2\alpha}$	$A_{3\alpha}$	M_β	P_α	X_α
A_{1-}	A_{2-}	A_{3-}	M_β	P_α	X_β	A_{1-}	$A_{2\alpha}$	$A_{3\alpha}$	M_β	P_α	X_β
A_{1-}	A_{2-}	A_{3-}	M_β	P_β	X_α	A_{1-}	$A_{2\alpha}$	$A_{3\alpha}$	M_β	P_β	X_α
A_{1-}	A_{2-}	A_{3-}	M_β	P_β	X_β	A_{1-}	$A_{2\alpha}$	$A_{3\alpha}$	M_β	P_β	X_β
A_{1-}	A_{2-}	A_{3-}	M_α	P_α	X_α	A_{1-}	$A_{2\alpha/\beta}$	$A_{3\beta/\alpha}$	M_α	P_α	X_α
A_{1-}	A_{2-}	A_{3-}	M_α	P_α	X_β	A_{1-}	$A_{2\alpha/\beta}$	$A_{3\beta/\alpha}$	M_α	P_α	X_β
A_{1-}	A_{2-}	A_{3-}	M_α	P_β	X_α	A_{1-}	$A_{2\alpha/\beta}$	$A_{3\beta/\alpha}$	M_α	P_β	X_α
A_{1-}	A_{2-}	A_{3-}	M_α	P_β	X_β	A_{1-}	$A_{2\alpha/\beta}$	$A_{3\beta/\alpha}$	M_α	P_β	X_β
A_{1-}	A_{2-}	A_{3-}	M_β	P_α	X_α	A_{1-}	$A_{2\alpha/\beta}$	$A_{3\beta/\alpha}$	M_β	P_α	X_α
A_{1-}	A_{2-}	A_{3-}	M_β	P_α	X_β	A_{1-}	$A_{2\alpha/\beta}$	$A_{3\beta/\alpha}$	M_β	P_α	X_β
A_{1-}	A_{2-}	A_{3-}	M_β	P_β	X_α	A_{1-}	$A_{2\alpha/\beta}$	$A_{3\beta/\alpha}$	M_β	P_β	X_α
A_{1-}	A_{2-}	A_{3-}	M_β	P_β	X_β	A_{1-}	$A_{2\alpha/\beta}$	$A_{3\beta/\alpha}$	M_β	P_β	X_β
A_{1-}	A_{2-}	A_{3-}	M_α	P_α	X_α	A_{1-}	$A_{2\alpha}$	$A_{3\alpha}$	M_α	P_α	X_α
A_{1-}	A_{2-}	A_{3-}	M_α	P_α	X_β	A_{1-}	$A_{2\alpha}$	$A_{3\alpha}$	M_α	P_α	X_β
A_{1-}	A_{2-}	A_{3-}	M_α	P_β	X_α	A_{1-}	$A_{2\alpha}$	$A_{3\alpha}$	M_α	P_β	X_α
A_{1-}	A_{2-}	A_{3-}	M_α	P_β	X_β	A_{1-}	$A_{2\alpha}$	$A_{3\alpha}$	M_α	P_β	X_β
A_{1-}	A_{2-}	A_{3-}	M_β	P_α	X_α	A_{1-}	$A_{2\alpha}$	$A_{3\alpha}$	M_β	P_α	X_α
A_{1-}	A_{2-}	A_{3-}	M_β	P_α	X_β	A_{1-}	$A_{2\alpha}$	$A_{3\alpha}$	M_β	P_α	X_β
A_{1-}	A_{2-}	A_{3-}	M_β	P_β	X_α	A_{1-}	$A_{2\alpha}$	$A_{3\alpha}$	M_β	P_β	X_α
A_{1-}	A_{2-}	A_{3-}	M_β	P_β	X_β	A_{1-}	$A_{2\alpha}$	$A_{3\alpha}$	M_β	P_β	X_β

The t_1 dimension corresponds to 3Q terms and t_2 dimension is the corresponding terms converted to SQ.

4.6. Homonuclear ^{13}C double-quantum (DQ)–SQ correlation experiment

In the homonuclear 3Q–SQ correlation experiments discussed earlier, the active spins have the same chemical shifts and are indistinguishable. On the other hand the two ^{13}C spins have distinguishable chemical shifts. Hence the possibility of unambiguous determination of relative signs of the couplings using homonuclear ^{13}C DQ–SQ correlation was explored. In one-dimensional fully coupled ^{13}C spectrum of isotopomer **4** reported in Fig. 1C, the carbon M of the A_3MPX spin system is split into a quartet by three protons

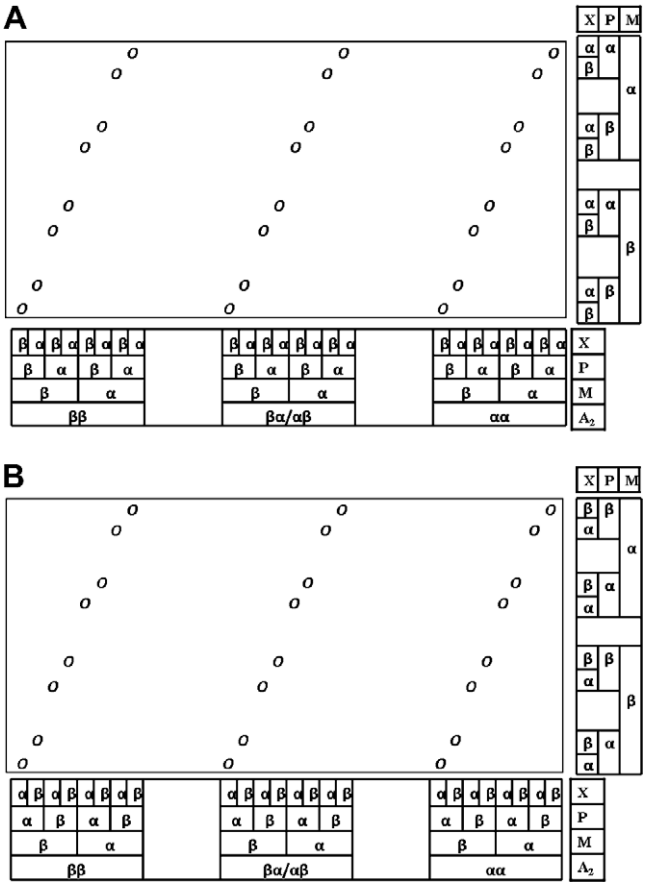

Fig. 7. (A) The pictorial representation of the homonuclear 3Q–SQ correlation spectrum of isotopomer **4**, with the assumption that all the passive couplings are of the same signs. 3Q dimension pertains to eight possible spin states of M, P and X. In the SQ dimension each proton resonance is split into a triplet from the remaining two protons giving rise to a triplet of intensity 1:2:1 corresponding to the $|\alpha\alpha\rangle$, $|\alpha\beta\rangle$, $|\beta\alpha\rangle$ and $|\beta\beta\rangle$ states. Each of these transitions is further split due to eight spin states of M, P and X as shown. Note for each spin state in the 3Q dimension, there is a triplet giving D_{HH} and the directions of the displacements due to all the couplings are the same. (B) The pictorial representation of the homonuclear 3Q–SQ correlation spectrum of isotopomer **4**, for different sign combinations of passive couplings. 3Q dimension pertains to eight possible spin states of M, P and X. The appearance of the spectrum is illustrated with an initial assumption that T_{15} and T_{16} are negative. Note for each spin state in the 3Q dimension, there is triplet giving information on D_{HH} and the direction of the displacement due to all the couplings are the same. Furthermore, the direction of the displacement vector is same in both (A) and (B).

(A_3), each of which further splits into doublet of doublets due to coupling to the other ^{13}C(P) and ^{15}N(X) spins, respectively. The spectrum for carbon P is more complex because of nearly equal values of T_{15},T_{45} and T_{56}.

The DQ excitation of two coupled carbon spins, converts the six spin system of the type A_3MPX into an A_3MX type in the DQ dimension, where the three protons (A_3) and ^{15}N (X) are passive spins and two carbons are active spins (M). The DQ detection corresponds to M part of this A_3MX spin system and the DQ states of two carbons, $|C_\alpha C_\alpha\rangle$ and $|C_\beta C_\beta\rangle$ are coupled to eight different spin states of methyl protons and two different spin states of ^{15}N. Thus DQ transition splits into a quartet due to the couplings to protons and each of these quartets are further split into a doublet due to ^{15}N spin. Fig. 8 shows the DQ–SQ spectrum along with the corresponding projections. The carbon 4 directly bonded to protons resonates at high field and also has large T_{14}. The carbon 5 remotely bonded to protons resonates at lower field and has smaller T_{15}. The cross section taken along SQ dimension at each spin state of a passive spin in the DQ dimension is a doublet from which T_{45} can be directly obtained. T_{14} can be determined from the combined

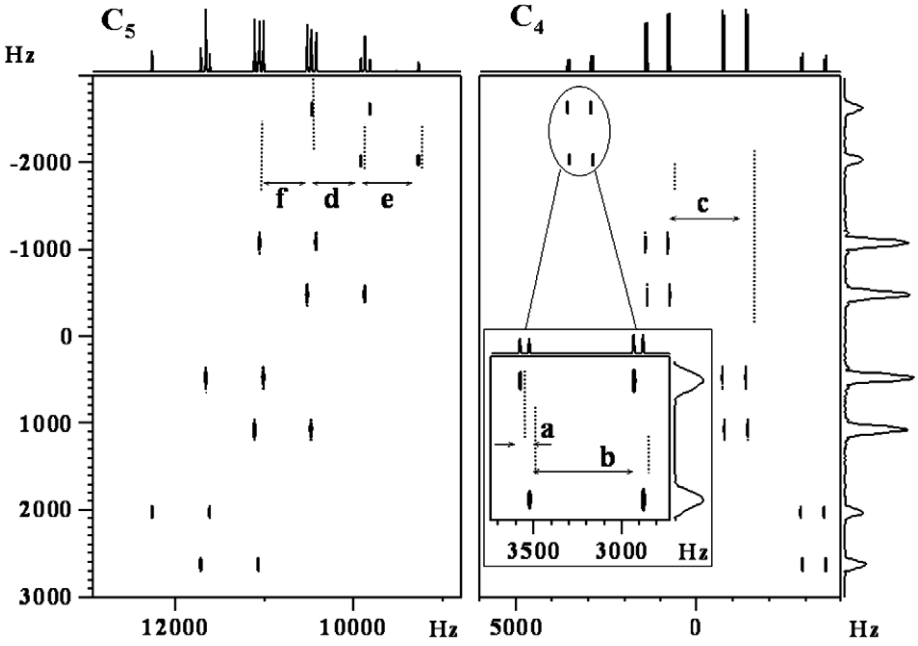

Fig. 8. The homonuclear ^{13}C DQ–SQ spectrum of isotopomer **4**. The t_1 and t_2 corresponds to DQ and SQ dimensions. The 2D data matrix is 256 × 8k. Sixteen scans for each FID was accumulated with a recycle delay of 5 s. The optimized τ delay was 0.4 ms. Digital resolution is 15.0 and 1.0 Hz in F_1 and F_2 dimensions, respectively. For better clarity of the displacement and the measure of small couplings, the small region of the spectrum is expanded for carbon 4 and shown in the inset.

analysis of any two consecutive cross sections. Similarly the analysis of the low-field region of the spectrum pertaining to cyanide carbon (C_5) provides T_{45} and T_{15}. From the figure it is clearly evident that the directions of displacement of quartets providing T_{14} and T_{15} are opposite to each other indicating that these two couplings are of opposite signs. Furthermore, the displacement of each component of the doublet providing T_{46} and T_{56} are in the same direction indicating T_{46} and T_{56} are of the same signs. Additionally, at the chemical shift position of C_4, the displacement of quartets due to T_{14} and the doublets due to T_{46} are in the same direction, indicating these couplings are of same signs. Similar displacements at the chemical shift position of C_5 are opposite indicating that T_{15} and T_{56} are of opposite signs. These observations contradict our previous results obtained using heteronuclear MQ–SQ experiments, i.e., T_{14} is positive; T_{46}, T_{15} and T_{56} are negative. The polarization operator formalism was employed again to understand the spin dynamics.

4.7. Spin dynamics in homonuclear ^{13}C DQ–SQ experiment

The two double-quantum states of the carbons M and P in the t_1 dimension corresponds to $|\alpha\alpha\rangle$ and $|\beta\beta\rangle$. The coherence between these two states is represented as M_+P_+. Therefore, the DQ operator during the t_1 period can be written as $A_{1i}A_{2j}A_{3k}M_+P_+X_l$, where i, j, k and l represent any of the $|\alpha\rangle$ and $|\beta\rangle$ states of three protons and X spin, respectively. Pertaining to 16 possible spin states of the pas-

Table 3
Evolution in homonuclear ^{13}C DQ–SQ correlation experiment on isotopomer **4**

T_1 period (DQ)						T_2 period (SQ)											
						M spin detected						P spin detected					
A_1	A_2	A_3	M	P	X	A_1	A_2	A_3	M	P	X	A_1	A_2	A_3	M	P	X
$A_{1\alpha}$	$A_{2\alpha}$	$A_{3\alpha}$	M_+	P_+	X_α	$A_{1\alpha}$	$A_{2\alpha}$	$A_{3\alpha}$	M_-	P_α	X_α	$A_{1\alpha}$	$A_{2\alpha}$	$A_{3\alpha}$	M_α	P_-	X_α
						$A_{1\alpha}$	$A_{2\alpha}$	$A_{3\alpha}$	M_-	P_β	X_α	$A_{1\alpha}$	$A_{2\alpha}$	$A_{3\alpha}$	M_β	P_-	X_α
$A_{1\alpha}$	$A_{2\alpha}$	$A_{3\alpha}$	M_+	P_+	X_β	$A_{1\alpha}$	$A_{2\alpha}$	$A_{3\alpha}$	M_-	P_α	X_β	$A_{1\alpha}$	$A_{2\alpha}$	$A_{3\alpha}$	M_α	P_-	X_β
						$A_{1\alpha}$	$A_{2\alpha}$	$A_{3\alpha}$	M_-	P_β	X_β	$A_{1\alpha}$	$A_{2\alpha}$	$A_{3\alpha}$	M_β	P_-	X_β
$A_{1\alpha}$	$A_{2\alpha}$	$A_{3\beta}$	M_+	P_+	X_α	$A_{1\alpha}$	$A_{2\alpha}$	$A_{3\beta}$	M_-	P_α	X_α	$A_{1\alpha}$	$A_{2\alpha}$	$A_{3\beta}$	M_α	P_-	X_α
						$A_{1\alpha}$	$A_{2\alpha}$	$A_{3\beta}$	M_-	P_β	X_α	$A_{1\alpha}$	$A_{2\alpha}$	$A_{3\beta}$	M_β	P_-	X_α
$A_{1\alpha}$	$A_{2\alpha}$	$A_{3\beta}$	M_+	P_+	X_β	$A_{1\alpha}$	$A_{2\alpha}$	$A_{3\beta}$	M_-	P_α	X_β	$A_{1\alpha}$	$A_{2\alpha}$	$A_{3\beta}$	M_α	P_-	X_β
						$A_{1\alpha}$	$A_{2\alpha}$	$A_{3\beta}$	M_-	P_β	X_β	$A_{1\alpha}$	$A_{2\alpha}$	$A_{3\beta}$	M_β	P_-	X_β
$A_{1\alpha}$	$A_{2\beta}$	$A_{3\alpha}$	M_+	P_+	X_α	$A_{1\alpha}$	$A_{2\beta}$	$A_{3\alpha}$	M_-	P_α	X_α	$A_{1\alpha}$	$A_{2\beta}$	$A_{3\alpha}$	M_α	P_-	X_α
						$A_{1\alpha}$	$A_{2\beta}$	$A_{3\alpha}$	M_-	P_β	X_α	$A_{1\alpha}$	$A_{2\beta}$	$A_{3\alpha}$	M_β	P_-	X_α
$A_{1\alpha}$	$A_{2\beta}$	$A_{3\alpha}$	M_+	P_+	X_β	$A_{1\alpha}$	$A_{2\beta}$	$A_{3\alpha}$	M_-	P_α	X_β	$A_{1\alpha}$	$A_{2\beta}$	$A_{3\alpha}$	M_α	P_-	X_β
						$A_{1\alpha}$	$A_{2\beta}$	$A_{3\alpha}$	M_-	P_β	X_β	$A_{1\alpha}$	$A_{2\beta}$	$A_{3\alpha}$	M_β	P_-	X_β
$A_{1\beta}$	$A_{2\beta}$	$A_{3\beta}$	M_+	P_+	X_α	$A_{1\beta}$	$A_{2\beta}$	$A_{3\beta}$	M_-	P_α	X_α	$A_{1\beta}$	$A_{2\beta}$	$A_{3\beta}$	M_α	P_-	X_α
						$A_{1\beta}$	$A_{2\beta}$	$A_{3\beta}$	M_-	P_β	X_α	$A_{1\beta}$	$A_{2\beta}$	$A_{3\beta}$	M_β	P_-	X_α
$A_{1\beta}$	$A_{2\beta}$	$A_{3\beta}$	M_+	P_+	X_β	$A_{1\beta}$	$A_{2\beta}$	$A_{3\beta}$	M_-	P_α	X_β	$A_{1\beta}$	$A_{2\beta}$	$A_{3\beta}$	M_α	P_-	X_β
						$A_{1\beta}$	$A_{2\beta}$	$A_{3\beta}$	M_-	P_β	X_β	$A_{1\beta}$	$A_{2\beta}$	$A_{3\beta}$	M_β	P_-	X_β

The t_1 dimension corresponds to DQ terms and t_2 dimension is the corresponding terms converted to SQ.

sive spins, there are eight transitions along the F_1 dimension at the chemical shift position of each carbon. The application of the second 90° pulse converts these DQ terms into SQ terms. As an example, the DQ term M_+P_+coupled to one of the passive spin states, viz., $A_{1\alpha}A_{2\alpha}A_{3\alpha}$ gets converted to M and P single-quantum terms as;

$$\begin{aligned} A_{1\alpha}A_{2\alpha}A_{3\alpha}M_+P_+X_\alpha \rightarrow\ & A_{1\alpha}A_{2\alpha}A_{3\alpha}M_-P_\alpha X_\alpha \\ & A_{1\alpha}A_{2\alpha}A_{3\alpha}M_-P_\beta X_\alpha \\ & A_{1\alpha}A_{2\alpha}A_{3\alpha}M_\alpha P_-X_\alpha \\ & A_{1\alpha}A_{2\alpha}A_{3\alpha}M_\beta P_-X_\alpha \end{aligned} \quad (2)$$

Similarly, the conversion of the DQ coherence coupled to all the remaining seven passive spin states can be worked out and are summarized in Table 3.

To understand the displacement of cross sections the 2D matrix was again pictorially depicted for different sign combinations. The Fig. 9A represents the spectrum when all the signs of passive couplings are the same and Fig. 9B represents the spectrum when the signs of T_{15}, T_{46} and $T_{56}$are reversed. This pertains to a situation when the spin states $|\alpha\rangle$ and $|\beta\rangle$ of M and P spins are interchanged in both DQ and SQ dimensions. Clearly Fig. 9A and B are not identical in appearance indicating that the information on the relative signs can be derived from this 2D matrix. This pictorial representation can be extended further for several combinations of signs of the couplings. All these representations reveal the possibility of obtaining the relative signs from the DQ–SQ experiment. Thus it is evident that one can determine the signs of the couplings by employing the direction of tilt of the displacement vectors in a situation when the active spins are distinguishable. Furthermore the comparison of the tilts of the displacement vectors is possible only when the passive spins are of the same type. This implies that for the determination of the relative signs of the couplings from the displacement vectors, the prerequisite is that the passive spins should be identical and the active spins should be distinguishable. With these conclusions, the correct signs and magnitudes of the couplings were determined and are reported in Table 1. The relative signs of the J_{ij} determined using these experiments have been utilized to determine the precise values and relative signs of dipolar couplings.

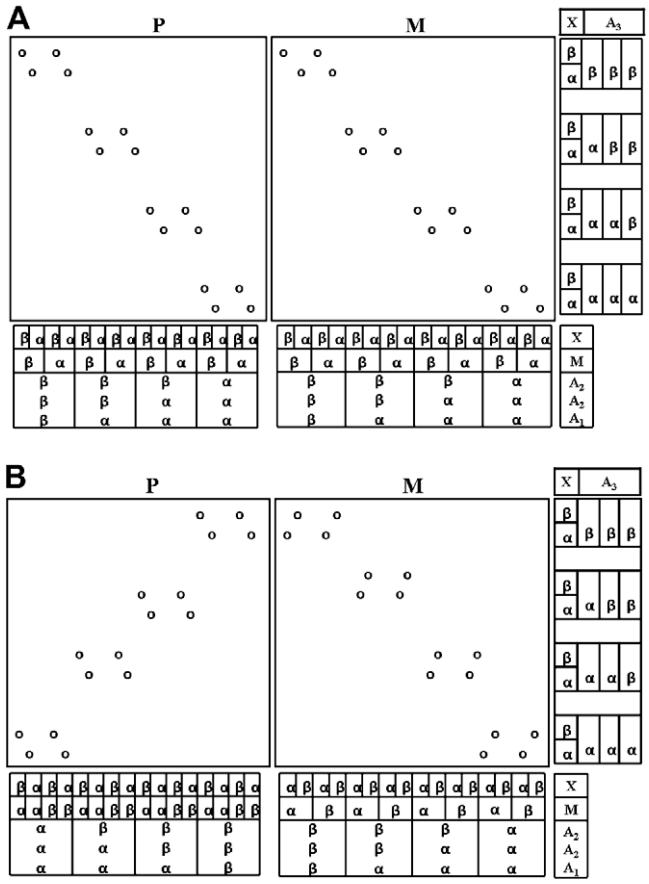

Fig. 9. (A) The pictorial representation of the homonuclear ^{13}C DQ–SQ correlation spectrum of isotopomer **4**, with the assumption that all the passive couplings are of same signs. The DQ dimension pertains to eight possible spin states of A_3 and X spins. Similarly in the SQ dimension each ^{13}C resonance is split into a doublet of a quartet from the three protons and ^{15}N spin. Each of the sixteen transitions at the chemical shift position of each carbon in the SQ dimension pertains to a particular spin state of three protons, the ^{13}C and ^{15}N spins. Note for each spin state in the DQ dimension, there is doublet giving information on T_{45} and the directions of the displacements due to all the couplings are the same. (B) The pictorial representation of the homonuclear ^{13}C DQ–SQ correlation spectrum of isotopomer **4**, for different sign combinations of passive couplings. The spectrum is represented by reversing the signs of T_{15}, T_{46} and T_{56}. Note for each spin state in the DQ dimension, there is doublet giving information on T_{45} and the direction of the displacement due to all the couplings are different.

4.8. MQ experiments on isotopomer *4* in isotropic phase

Relative signs of the scalar couplings are obtainable in the isotropic medium from identical experiments discussed above. By appropriate combination of three experiments, viz., $^{13}C_4$–$^{13}C_5$ $^{13}C_4$–^1H and $^{15}N_6^1H$ double quantum, all the signs and magnitudes of scalar couplings have been determined.

As discussed for the oriented acetonitrile, the directions of the displacement vectors can be utilized to extract the signs of the couplings in a conventional way without taking the sign of the gyromagnetic ratio into account. The ^{13}C–^{13}C DQ experiment reported in Fig. 10 shows that the signs of $^1J_{C_4H}$ and $^2J_{C_5H}$ are opposite and $^2J_{C_4N_6}$ and $^1J_{C_5N_6}$ have the same signs. Assuming $^1J_{C_4H}$ to be positive we can conclude that $^2J_{C_5H}$ is negative. Similarly the splittings along the MQ dimension in heteronuclear $^{13}C_4$–^1H DQ experiment (Fig. 11) shows that $^1J_{C_4C_5}$ and $^2J_{C_5H}$ are of opposite signs. From these two experiments it is obvious that $^1J_{C_4C_5}$ is positive. Furthermore, the smaller splitting along the MQ dimension shows that $^2JC_4N_6$ and $^3J_{N_6H}$ are of opposite signs. Also the $^{15}N_6$–^1H DQ spectrum (Fig. 12) provides the information that $^1J_{C_4H}$ and $^1J_{C_4N_6}$ are of opposite signs. In addition the experiment also depicts that $^2J_{C_5H}$ and $^1J_{C_5N_6}$ are of opposite signs. Employing these experiments the information on the relative signs of all the couplings have been determined and are reported Table 1. The signs of these couplings are in agreement with the previous reports [32,33].

4.9. Use of molecular geometry for confirming the relative signs

Taking into account the fixed geometry of acetonitrile [1], assuming a single-order parameter and positive sign for D_{HH}, the magnitudes and signs of the dipolar couplings were calculated. Experimental results agree with these values and are reported in Table 1.

5. Conclusions

The spin-selective and non-selective homo- and heteronuclear multiple quantum–single-quantum correlation experiments have been carried out. The methodology is employed for simultaneous and/or selective decoupling of different heteronuclei for spectral simplification. In the spin-selective experiments, the states of passive spins do not get disturbed both in the MQ and in the SQ dimensions providing the spin state selection. The tilt of the displacement of the cross sections in the F_1 dimension of the spin state selected spectra provides the relative signs be-

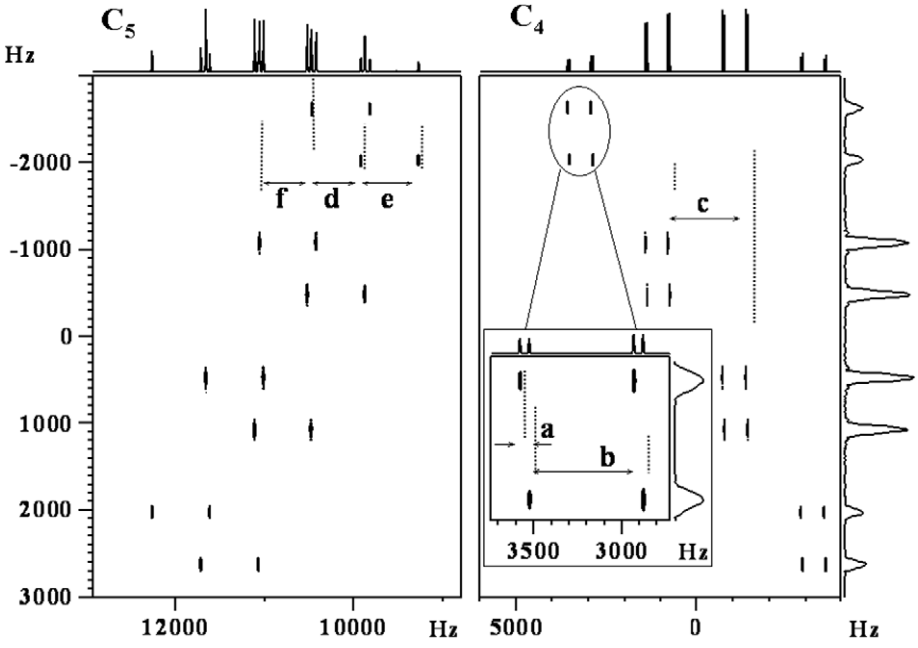

Fig. 10. The homonuclear ^{13}C DQ–SQ spectrum of doubly labeled acetonitrile (isotopomer **4**) in isotropic phase. The t_1 and t_2 corresponds to DQ and SQ dimensions. The 2D data matrix is 512 × 8k. Eight scans for each FID was accumulated with a recycle delay of 5 s. The optimized τ delay was 4.3 ms. Digital resolution was 1.0 and 0.5 Hz in F_1 and F_2 dimensions, respectively. Arrows depict the opposite directions of displacements of J_{14} and J_{15} and J_{46} and J_{56}, respectively. These pairs have been identified by the bent arrows.

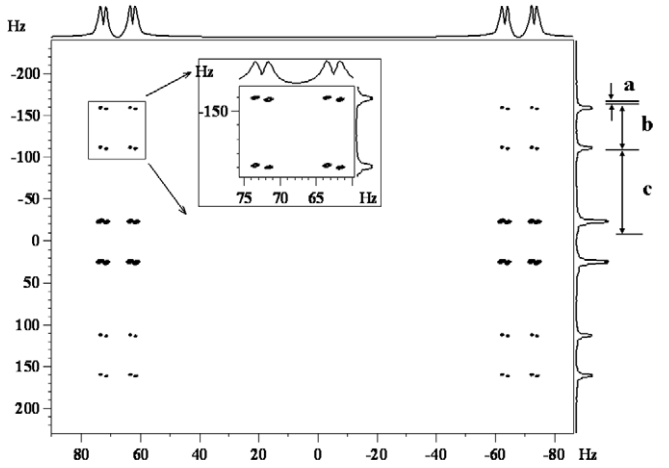

Fig. 11. The heteronuclear A_3M DQ spectrum of doubly labeled acetonitrile (isotopomer **4**) in isotropic phase. The t_1 and t_2 corresponds to DQ and SQ dimensions. The 2D data matrix is 128 × 4k. Four scans for each FID were accumulated and a recycle delay of 3 s. The optimized τ delay was 1.8 ms. Digital resolution was 0.4 and 0.1 Hz in F_1 and F_2 dimensions, respectively. The separations (in Hz) provide (a) $J_{16} \pm J_{46}$, (b) $J_{15} \pm J_{45}$ and (c) J_{14}. The direction of the displacement is obvious from the expanded region of the spectrum is shown in the inset.

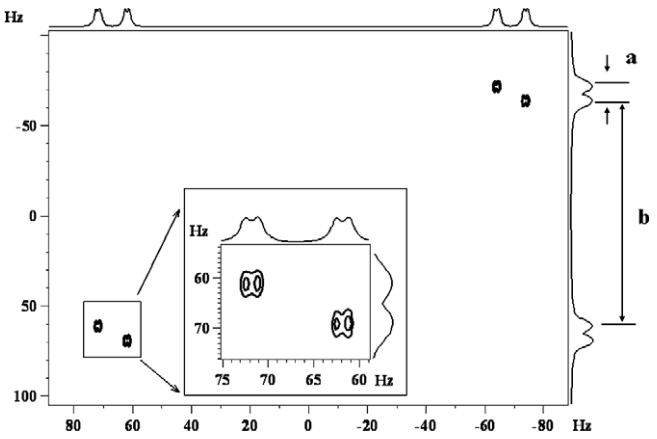

Fig. 12. The heteronuclear A_3X DQ spectrum of doubly labeled acetonitrile (isotopomer **4**) in isotropic phase. The t_1 and t_2 corresponds to DQ and SQ dimensions. The 2D data matrix is 128 × 4k. Four scans for each FID were accumulated and a recycle delay of 3 s. The optimized τ delay was 125 ms. Digital resolution was 1.0 and 0.2 Hz in F_1 and F_2 dimensions, respectively. The separations (in Hz) provide (a) $^1J)C_4H \pm {}^1J_{C_4N_6}$ and (b) $^2J_{C_5H} \pm {}^1J_{C_5N6}$. The expanded region of the spectrum is shown in the inset.

tween the active and passive couplings in addition to their magnitudes. However, one can encounter ambiguous situations in the determination of the relative signs of the couplings. The dynamics of the spin system for different MQ–SQ correlation experiments have been understood using polarization operator approach. Both ambiguous and unambiguous situations in deriving the relative signs of the couplings have been discussed. It is observed that the pre-requisite for unambiguous determination of the relative signs of the couplings is that, the active spins flipped for MQ excitation should be distinguishable and the passive spins should be identical. The validity of the experiments has been confirmed both in the isotropic phase and also by molecular geometry calculations.

Acknowledgment

N.S. gratefully acknowledges the financial support by Department of Science and Technology, New Delhi, for the Grant No. SR/S1/PC-13/2004.

References

[1] J.W. Emsley, J.C. Lindon, NMR Spectroscopy Using Liquid Crystal Solvents, Pergamon Press, Oxford, 1975.
[2] J. Jeener, Ampere Summer School, Basko Polje, Yugoslavia, 1971.
[3] P. Aue, E. Bartholdi, R.R. Ernst, Two-dimensional spectroscopy. Application to nuclear magnetic resonance, J. Chem. Phys. 64 (1976) 2229–2246.
[4] W.H. Oschkinat, A. Pastore, P. Pfändler, G. Bodenhausen, Two-dimensional correlation of directly and remotely connected transitions by z-filtered COSY, J. Magn. Reson. 69 (1986) 559.

[5] R. Brüschweiler, J.C. Madsen, C. Griesinger, O.W. Sørensen, R.R. Ernst, Two-dimensional NMR spectroscopy with soft pulses, J. Magn. Reson. 73 (1987) 380.
[6] C. Griesinger, O.W. Sørensen, R.R. Ernst, Two-dimensional correlation of connected NMR transitions, J. Am. Chem. Soc. 107 (1985) 6394.
[7] R. Freeman, The relative signs of NMR spin coupling constants from double irradiation experiments, Mol. Phys. 4 (1961) 385.
[8] W.S. Brey, L.W. Jaques, H.J. Jakobsen, A $^{13}C-^{1}H$ double resonance study of the signs of $^{1}H-^{19}F$ and $^{13}C-^{19}F$ spin coupling constants in fluorobenzenes and 2-fluoropyridine, Org. Magn. Reson. 12 (1979) 243.
[9] P. Permi, S. Heikkinen, I. Kilpeläinen, A. Annila, Measurement of homonuclear ^{2}J-couplings from spin-sate selective double-/zero-quantum two-dimensional NMR spectra, J. Magn. Reson. 139 (1999) 273.
[10] G. Otting, A DQ/ZQ NMR experiment for the determination of the signs of small $J(^{1}H, ^{13}C)$ coupling constants in linear spin systems, J. Magn. Reson. 124 (1997) 503.
[11] A. Rexroth, P. Schmidt, S. Szalma, T. Geppert, H. Schwalbe, C. Griesinger, New principle for the determination of coupling constants that largely suppresses differential relaxation effects, J. Am. Chem. Soc. 117 (1995) 10389.
[12] P. Anderson, J. Weigelt, G. Otting, Spin-state selection filters for the measurement of heteronuclear one-bond coupling constants, J. Biomol. NMR 12 (1988) 435.
[13] B. Brutscher, Accurate measurement of small spin–spin couplings in partially aligned molecules using a novel *J*-mismatch compensated spin-state-selection filter, J. Magn. Reson. 151 (2001) 332.
[14] P. Permi, Determination of three-bond scalar couplings between $^{13}C'$ and $^{1}H^{\alpha}$ in protein using an *i*HN(CA),CO(α/β-*J*-COHA) experiment, J. Magn. Reson. 163 (2003) 114.
[15] L . Duma, S. Hediger, A. Lesage, L. Emsley, Spin-state selection in solid-state NMR, J. Magn. Reson. 164 (2003) 187.
[16] L. Duma, S. Hediger, B. Brutscher, A. Böckmann, L. Emsley, Resolution enhancement in multidimensional solid-state NMR spectroscopy of proteins using spin-state selection, J. Am. Chem. Soc. 125 (2003) 11816.
[17] P. Nolis, J.F. Espinosa, T. Parella, Optimum spin-state selection for all multiplicities in the acquisition dimension of the HSQC experiment, J. Magn. Reson. 180 (2006) 39.
[18] R. Verel, T. Manolikas, A.B. Siemer, B.H. Meier, Improved resolution in ^{13}C solid-state spectra through spin-state-selection, J. Magn. Reson. 184 (2007) 322.
[19] P. Permi, A. Annila, A new approach for obtaining sequential assignment of large proteins, J. Biomol. NMR 20 (2001) 127.
[20] P. Permi, A. Annila, Transverse relaxation optimized spin-state selective NMR experiments for measurement of residual dipolar couplings, J. Biomol. NMR 16 (2000) 221.
[21] P. Permi, A spin-state-selective experiment for measuring heteronuclear one-bond and homonuclear two-bond couplings from an HSQC-type spectrum, J. Biomol. NMR 22 (2002) 27.
[22] D. Lee, B. Vögeli, K. Pervushin, Detection of C′, C_{α}correlations in proteins using a new time- and sensitivity optimal-experiment, J. Biomol. NMR 31 (2005) 273.
[23] P. Würtz, K. Fredriksson, P. Permi, A set of HA-detected experiments for measuring scalar and residual dipolar couplings, J. Biomol. NMR 31 (2005) 321.
[24] P. Nolis, T. Parella, Simultaneous spin-state α/β selection for ^{13}C and ^{15}N from a time-shared HSQC-IPAP experiment, J. Biomol. NMR 37 (2007) 65.
[25] B. Bikash, N. Suryaprakash, Spin state selective detection of single quantum transitions using multiple quantum coherence: simplifying the analyses of complex NMR spectra, J. Phys. Chem. A 111 (2007) 5211.
[26] B. Bikash, N. Suryaprakash, Spin selective multiple quantum NMR for spectral simplification, determination of relative signs, and magnitudes of scalar couplings by spin state selection, J. Chem. Phys. 127 (2007) 214510.
[27] L. Braunschweiler, G. Bodenhausen, R.R. Ernst, Analysis of networks of coupled spins by multiple quantum NMR, Mol. Phys. 48 (1983) 535.
[28] W.S. Warren, A. Pines, Analogy of multiple-quantum NMR to isotopic spin labeling, J. Am. Chem. Soc. 103 (1981) 1613.
[29] W.S. Warren, D.P. Weitekamp, A. Pines, Theory of selective excitation of multiple-quantum transitions, J. Chem. Phys. 73 (1980) 2084.
[30] L.D. Field, G.K. Pierens, T.A. Carpenter, L.D. Colebrook, L.D. Hall, Selection of multiple quantum spectra of molecules in liquid crystalline solution using pulsed magnetic field gradients, J. Magn. Reson. 99 (1992) 398.
[31] J. Keeler, Understanding NMR Spectroscopy, John Wiley and Sons, England, 2005.
[32] G. Englert, A. Saupe, Molecular geometry of acetonitrile, determined by proton magnetic resonance in nematic solutions, Mol. Cryst. Liq. Cryst. 8 (1969) 233.
[33] O.W. Sørensen, H. Bildsøe, H. Jakobsen, Natural-abundance proton-coupled satellite spectra in ^{13}C NMR from double selective population transfer. The flip angle effect, J. Magn. Reson. 45 (1981) 325.